This full text paper was peer reviewed at the direction of IEEE Communications Society subject matter experts for publication in the ICC 2008 proceedings.

Near-Capacity Irregular Precoded Linear Dispersion Codes

Nan Wu
School of ECS, University of Southampton
SO17 1BJ, UK
nw04r@ecs.soton.ac.uk
http://www-mobile.ecs.soton.ac.uk/newcomms/

Lajos Hanzo
School of ECS, University of Southampton
SO17 1BJ, UK
lh@ecs.soton.ac.uk
http://www-mobile.ecs.soton.ac.uk/newcomms/

***Abstract*—In this treatise, we propose a novel serial concatenated RSC-coded Irregular Precoded Linear Dispersion Codes (IR-PLDC), which is capable of operating near MIMO channel's capacity. The irregular structure combined with the employment of an Infinite Impulse Response (IIR) precoder facilities the proposed system's operation across a wide range of SNRs, while maintaining an infinitesimally low BER. Each coding block of the IR-PLDC scheme is designed with near-capacity operation in mind with the aid of Extrinsic Information Transfer (EXIT) charts. The proposed RSC-coded IR-PLDC scheme is capable of operating as close as 2.5dB to the MIMO channel's capacity, namely at SNRs as low as $\rho = -7$dB.**

I. INTRODUCTION

Wireless communication systems using multiple antennas at both the transmitter and receiver, which are referred to as a Multiple Input and Multiple Output (MIMO) systems in the literature, have the potential of maintaining reliable wireless transmissions at high data rates [1], [2]. The design of coding schemes for MIMO systems operating at high Signal-to-Noise Ratios (SNRs) involves a tradeoff between the achievable rate at which the system's capacity increases and the rate at which the error probability decays [3]. There is considerable interest in developing schemes that provide different trade-offs in terms of the achievable rate and error probability, which are applicable for employment in a broad range of antenna configurations.

The set of Linear Dispersion Codes (LDCs), first proposed by Hassibi and Hochwald [4], constitutes a wide-ranging class of space-time codes exhibiting diverse characteristics. Hence this family encompasses numerous existing schemes, providing a natural framework in which such design problems can be posed. The revolutionary concept of LDCs [4] [5] invokes a matrix-based linear modulation framework, where each space-time transmission matrix is generated by a linear combination of so-called dispersion matrices and the weights of the components are determined by the transmitted symbols. The dispersion matrices were originally designed for maximizing the ergodic capacity [1] of the resultant equivalent MIMO system. However, the LDCs proposed in [4] did not necessarily guarantee a low Bit Error Ratio (BER) [5] [6].

Serial Concatenated Codes (SCC) are capable of attaining an infinitesimally low BER, while maintaining a manageable decoding complexity [7] [8]. Since LDCs have the ability to approach the potential capacity of MIMO systems, it is natural to serially concatenate for example a simple convolutional channel code as the outer code and LDCs employed as the inner code in order to approach the MIMO capacity, while maintaining a near error-free BER performance.

It has been demonstrated in [9] [10] that SCCs benefit from having an open convergence tunnel at low SNRs, when IrRegular Convolutional Codes (IRCCs) were adopted as the outer channel code, since IRCCs exhibited flexible Extrinsic Information Transfer (EXIT) chart characteristics [9] [10]. However, SCCs employing irregular outer codes are unable to operate at low SNRs, where the associated convergence tunnel is closed. Furthermore, near-capacity IRCC schemes may require an excessive number of iterations at the receiver to achieve an infinitesimally low BER, which may exceed the affordable complexity budget of mobile handsets. The potentially high decoding delay also constitutes a problem associated with IRCC schemes, owing to the requirement of having a high interleaver length.

Motivated by the above-mentioned flexibility of the irregular outer code design philosophy, in this treatise we circumvent the IRCC-related outer code limitations by proposing IrRegular Precoded Linear Dispersion Codes (IR-PLDCs) as inner rather than outer code and serially concatenate the resultant IR-PLDCs with a low-complexity regular outer channel code in order to achieve an infinitesimally low BER, when employing iterative decoders. The rationale and novelty of the proposed iterative detected IR-PLDCs are:

- We propose IR-PLDC schemes as the inner code of SCCs, which are capable of achieving an infinitesimally low BER across a wide range of SNRs;
- We investigate the maximum achievable rate of the IR-PLDCs with the aid of EXIT charts [11] [12], when using Minimum Mean Squared Error (MMSE) detectors;
- LDCs are optimized by maximizing the Discrete-input Continuous-output Memoryless Channel's (DCMC) capacity;
- IR-PLDCs may be reconfigured by activating different dispersion matrices for the different component codes at a modest hardware cost;
- IR-PLDCs can be designed for an arbitrary number of transmit as well as receive antennas and combined with arbitrary modulation schemes.

We commence our discourse by providing a detailed description of the proposed IR-PLDC system's structure in Section II. In Section III, we demonstrate how the proposed irregular inner code system is constructed from a capacity maximization perspective. Our simulation results are discussed in Section IV. Finally, we conclude our discourse in Section V.

II. SYSTEM DESCRIPTION

We consider a MIMO system employing M transmit as well as N receive antennas and Figure 1 portrays the system model of the proposed serially concatenated RSC-coded IR-PLDC scheme. At the transmitter, a frame of information bits u_1 is encoded by a simple RSC encoder. Then the encoded bits c_1 are interleaved by a random interleaver, yielding the outer encoded bits u_2. Then the "irregular partitioner" of Figure 1 feeds the appropriately selected fraction of u_2 into the various Precoded LDC (PLDC) component codes, according to the predefined weighting coefficient vector $\boldsymbol{\lambda} = [\lambda_1, \cdots, \lambda_P]$, where P denotes the total number of PLDC components. Memory-1 unity-rate precoders were employed for all the PLDC components. More explicitly, within each PLDC encoder, the resultant precoded bits c_2 are interleaved by a second interleaver, yielding the interleaved bits u_3, which are fed to the bit-to-symbol mapper inside the LDC block of Figure 1. After modulation, the information bearing vector $\mathbf{K} = [s_1, \cdots, s_Q]$ containing Q L-PSK symbols is dispersed according to the space-time block matrix $\mathbf{S}$ of Equation (1) by the "ST mapper", spanning M spatial- and T temporal-dimensions. More

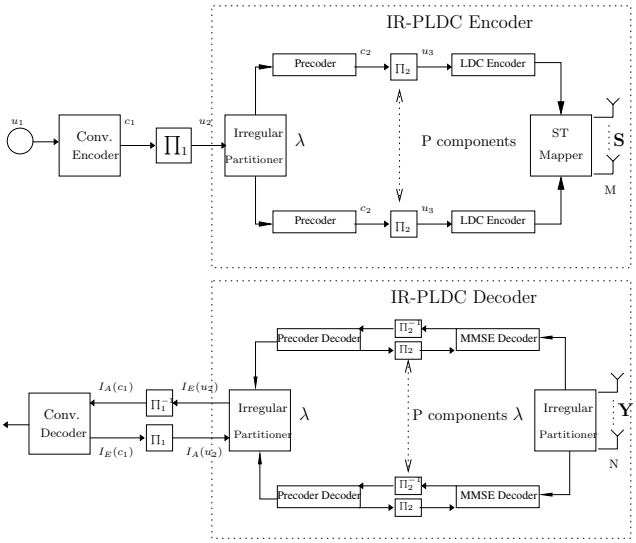

Figure 1. Schematic of the RSC-coded IR-PLDC with iterative decoding.

explicitly, **S** is given by:

$$\mathbf{S} = \sum_{q=1}^{Q} \mathbf{A}_q s_q, \qquad q = 1, \cdots, Q, \tag{1}$$

where $\mathbf{A}_q$ represents the corresponding dispersion matrix. Hence **S** is transmitted over the uncorrelated Rayleigh fading channel contaminated by AWGN at each receive antenna. The rate of a LDC is defined as:

$$R_{LDC} = \frac{Q}{T} \qquad (sym/slot). \tag{2}$$

At the receiver, the received signal matrix **Y** is related to **S** by:

$$\mathbf{Y} = \sqrt{\frac{\rho}{M}}\mathbf{H}\mathbf{S} + \mathbf{V}, \tag{3}$$

where the Channel Impulse Response (CIR) matrix **H** is modelled as independent and identically distributed (i.i.d.) flat Rayleigh fading and its envelope and phase are assumed to be constant during T symbol periods, while changing independently from one space-time matrix to the next. The CIR matrix **H** is assumed to be known to the receiver, but not to the transmitter. The noise matrix **V** is assumed to have independent samples of a zero-mean complex-valued Gaussian random process with a common variance of N_0 determined by the SNR ρ.

It is desirable to rewrite the input-output matrix relationship of Equation (3) in an equivalent vectorial form. Define the $vec()$ operation as the vertical stacking of the columns of an arbitrary matrix. Subjecting both sides of Equation (3) to the $vec()$ operation gives the equivalent system matrix [5]:

$$\bar{\mathbf{Y}} = \sqrt{\frac{\rho}{M}}\bar{\mathbf{H}}\chi\mathbf{K} + \bar{\mathbf{V}}, \tag{4}$$

where $\bar{\mathbf{Y}} \in \zeta^{NT\times 1}$, $\bar{\mathbf{H}} \in \zeta^{NT\times MT}$, $\chi \in \zeta^{MT\times Q}$, $\mathbf{K} \in \zeta^{Q\times 1}$ and $\bar{\mathbf{V}} \in \zeta^{NT\times 1}$. More explicitly, χ is referred to as the **Dispersion Character Matrix** (DCM), which is defined as

$$\chi = [vec(\mathbf{A}_1), vec(\mathbf{A}_2), \cdots, vec(\mathbf{A}_Q)], \tag{5}$$

while $\bar{\mathbf{H}}$ in Equation (4) is given by:

$$\bar{\mathbf{H}} = \mathbf{I}_T \otimes \mathbf{H}, \tag{6}$$

where $\otimes$ denotes the Kronecker product and $\mathbf{I}_T$ is the identity matrix having a size of $(T \times T)$. Note that the DCM χ uniquely and unambiguously determines a particular LDC$(MNTQ)$.

Again, the "irregular partitioner" of Figure 1 determines the specific portion of the received signal as well as the *a-priori* information $I_A(u_2)$ to be detected by each PLDC component decoder of the IR-PLDC scheme, according to the weighting coefficient vector $\boldsymbol{\lambda}$. Then, an iterative decoding structure is employed, where extrinsic information is exchanged between the three Soft-In Soft-Out (SISO) modules, namely the MMSE detector, the precoder and the outer RSC decoder in a number of consecutive iterations. To be specific, in Figure 1, $I_A()$ denotes the *a-priori* information represented in terms of Log-Likelihood Ratios (LLRs), where $I_E()$ denotes the extrinsic information also expressed in terms of LLRs. Note that the intermediate rate-1 precoder processes two *a-priori* inputs, namely those arriving from the MMSE detector as well as from the outer decoder and generates two extrinsic outputs. More detailed discussions on the iterative decoding process are provided in [7]. It is worth mentioning that the activation of different PLDC components is implemented by employing different dispersion matrices and the associated hardware cost is modest, since it does not require the implementation of P separate component codes at both the transmitter and receiver.

III. EXIT CHART BASED DESIGN OF IR-PLDCs

In our forthcoming EXIT chart analysis, the unity-rate precoder's decoder and the MMSE decoder are considered as a single 'inner' decoding block, constituted by the IR-PLDC's decoder seen in Figure 1. The advantage of this representation is that the IR-PLDC block's extrinsic information output $I_E(u_2)$ is only determined by the received signal matrix **Y** and the *a-priori* input $I_A(u_2)$, but remains unaffected by the extrinsic information exchange between the precoder's decoder and the MMSE detector. Thus, we can project the three-stage system into a two-stage system and hence the traditional two-dimensional EXIT charts [12] [13] are applicable.

Following the approach of [14], we now carry out the EXIT chart analysis of the proposed IR-PLDC system. Thus the corresponding EXIT transfer functions are:

$$I_E(u_2) = \Gamma_{in}[I_A(u_2), \rho]. \tag{7}$$

The employment of irregular codes was proposed by Tüchler and Hagenauer [9] [10], where IRCCs were used as an outer channel code. In [9], the authors have shown that the aggregate EXIT function of an irregular code containing P component codes can be obtained from the linear combination of that of its component codes, under the assumption that the Probability Density Function (PDF) of the LLRs is symmetric and continuous. More explicitly, the EXIT function of the proposed inner IR-PLDC scheme is given by:

$$\Gamma_{in} = \sum_{i=1}^{P} \lambda_i \Gamma_i(I_{in}, \rho), \tag{8}$$

where the weighting coefficient λ_i quantifies the particular fraction of the input bit stream that is encoded by the i-th component code and Γ_i denotes the EXIT function of the i-th PLDC component.

In the following sections, we will characterize each coding block of the IR-PLDC scheme of Figure 1 using various parameters, which are optimized from a capacity maximization perspective with the aid of EXIT charts.

A. Generating LDC Component codes

In this section, we demonstrate how to generate an inner IR-PLDC coding scheme containing $P = 12$ components for a MIMO configuration having $M = 2$ transmit and $N = 2$ receive antennas, when QPSK modulation was employed. It has been shown in [5] that the maximum achievable spatial diversity order of a LDC$(MNTQ)$ is $N \cdot \min(M, T)$. We commence by setting $T = M = 2$ for the first component. Hence, it has the potential of achieving the maximum diversity order of $D = 4$. By setting $Q = 1$, we are able to search

Table I
THE $P = 12$ COMPONENT CODES OF THE IR-PLDC SCHEME OF FIGURE 1 GENERATED FOR A MIMO SYSTEM HAVING $M = 2$ TRANSMIT AND $N = 2$ RECEIVE ANTENNAS.

Index	M	N	T	Q	**Rate**	D	j	**Complexity**
0	2	2	2	1	0.5	4	0	1571
1	⋮	⋮	⋮	2	1	4	1	4086
2	⋮	⋮	⋮	3	1.5	4	1	5030
3	⋮	⋮	⋮	4	2	4	1	5974
4	⋮	⋮	3	1	0.33	4	0	3285
5	⋮	⋮	⋮	2	0.67	4	1	8562
6	⋮	⋮	⋮	4	1.33	4	1	12546
7	⋮	⋮	⋮	5	1.67	4	1	14538
8	⋮	⋮	4	1	0.25	4	0	5639
9	⋮	⋮	⋮	3	0.75	4	1	18126
10	⋮	⋮	⋮	5	1.25	4	1	24974
11	⋮	⋮	⋮	7	1.75	4	1	31822

for the specific DCM χ, which maximizes the DCMC capacity of LDC(2221) using [15]:

$$C_{LDC}^{ML} = \frac{1}{T} \max_{p(K_1),\cdots,p(K_F)} \sum_{f=1}^{F} \int_{-\infty}^{\infty} \cdots \int_{-\infty}^{\infty} p(\mathbf{Y}|K_f) \cdot p(K_f) log_2 \left(\frac{p(\mathbf{Y}|K_f)}{\sum_{g=1}^{F} p(\mathbf{Y}|K_g) p(K_g)} \right), (bits/sym/Hz) \quad (9)$$

where K_f denotes all the possible transmitted vectors, each constituted by the Q transmitted symbols of $\mathbf{K}$, where we have a total $F = L^Q$ number of possibilities.

Consequently, we can obtain more components by gradually increasing the value of Q in order to increase the rate. We impose the limit of $Q \leq MT$ for the sake of maintaining a low complexity, although employing a higher value of Q is feasible. Hence, by increasing the value of T and maximizing the corresponding DCMC capacity of each LDC$(MNTQ)$, we can generate a set of meritorious LDCs. Naturally, low Q and T values are desirable for the sake of maintaining a low complexity. The resultant $P = 12$ component codes designed for our IR-PLDC scheme are listed in Table I.

The complexity of each PLDC component code is jointly determined by the precoder's memory, the MMSE detector's complexity and the number of inner iterations j. In order to quantify the complexity in a unified manner, we count the number of addition and multiplication operations required to calculate a single LLR value in the logarithmic domain. Since the number of addition and multiplication operations can be quantified in terms of the so-called Add-Compare-Select (ACS) arithmetic operations, the complexity of each PLDC component is quantified by the ACS operations per LLR computation. Observe in Table I that when the value of T is fixed, the complexity is increased by increasing the value of Q. Furthermore, increasing the value of T typically resulted in a substantially increased complexity.

B. The number of inner iterations

The number of 'inner' iterations between the MMSE detector and the precoder required for each PLDC component of Table I is also optimized for the sake of achieving the maximum capacity.

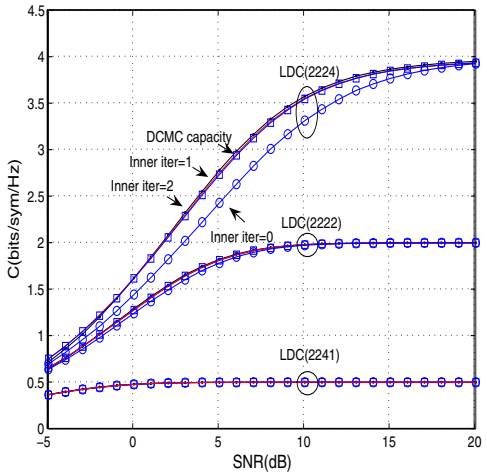

Figure 2. Comparison of the maximum achievable rates for the various PLDC schemes of Table I having $j = 0, 1, 2$ inner iterations, when using QPSK modulation in conjunction with an MMSE detector.

The so-called area property [13] [16] of EXIT charts may be formulated by stating that the area under the 'outer' RSC curve is approximately equal to its code rate R_{out}. Thus, if we assume that the area under the EXIT curve of an outer code can be perfectly matched to the area under the inner code's EXIT curve at any SNR, then it is possible to approximate the **maximum achievable rate** of a serial concatenated scheme by evaluating the area under the EXIT curves, given the rate of the 'inner' IR-PLDC code R_{in}, which is expressed as:

$$C(\rho) = log_2(L) \cdot R_{in} \cdot R_{out}, (bits/sym/Hz) \quad (10)$$

when L-PSK modulation is used.

Figure 2 quantifies the maximum achievable rates for the different PLDC components of Table I using different number of inner iterations j. For each set of comparisons, the DCMC capacity of the LDC using Equation (9) is plotted as a benchmarker. For the rate $R_{3,2224} = 2$ PLDC(2224) scheme, we observe a clear gap between the DCMC capacity and the corresponding maximum rate, when the number of inner iterations is $j = 0$. However, when we have $j = 1$, the aforementioned rate loss is eliminated and a further increase of the number of inner iterations j has only a modest additional rate improvement. In fact, the maximum achievable rate loss is less than 1%, when we have $j = 1$. For the PLDC(2222) scheme of Table I having a rate of $R_{1,2222} = 1$, we observe in Figure 2 that although the aforementioned maximum achievable rate loss compared to the DCMC capacity is still present, when employing $j = 0$ inner iterations, the associated discrepancy is narrower than that seen for the PLDC(2224) scheme. Observe in Figure 2 for the PLDC(2241) scheme having a rate of $R_{8,2241} = 0.25$ that there is no maximum achievable rate loss even in the absence of inner iterations.

The above observations are related to the EXIT characteristics of the LDC MMSE decoding block. When a single symbol is transmitted, the resultant EXIT curve is a horizontal line, which is a property of the Gray labelling employed [8]. Therefore, regardless of the number of inner iterations employed, the MMSE detector of Figure 1 always outputs the same extrinsic information. When Q is increased, the resultant EXIT curve become more steep, therefore higher extrinsic information can be obtained upon increasing the *a-priori* information by using a higher number of inner iterations. Therefore, the resultant maximum achievable rate observed in Figure 2 has an increasing discrepancy with respect to the DCMC

capacity, when a higher number of symbols Q is transmitted by each LDC block. We observe that for the component PLDCs of Table I, where we have $Q > 1$, employing $j = 1$ inner iteration will enable the system to attain 99% of the DCMC capacity.

C. Optimizing the weighing coefficient vector

Apart from the specific shape of the component EXIT curves, the aggregate IR-PLDC scheme's EXIT curve characterized in Equation (8) is also affected by the weighting coefficients, where λ_i, $i = (1, 2, \cdots, P)$ represents the specific fraction of the information bits fed into the IR-PLDC encoder/decoder of Figure 1. Therefore, the weighting coefficients $\boldsymbol{\lambda}$= $[\lambda_1, \cdots, \lambda_P]$ have to satisfy:

$$1 = \sum_{i=1}^{P} \lambda_i \qquad \lambda_i \in [0, 1], \tag{11}$$

and the resultant rate R_{in} of the inner IR-PLDC is given by:

$$\frac{1}{R_{in}} = \sum_{i=1}^{P} \lambda_i \frac{1}{R_{(i,LDC)}}, \tag{12}$$

where unity-rate precoders were employed.

In order to achieve an infinitesimally low BER at a specific SNR ρ, an open EXIT tunnel has to be maintained in the EXIT chart. Assuming that each component code's EXIT curve is represented by l points, the weighted irregular EXIT function Γ_{in} of the IR-PLDC at SNR ρ should be optimized by **maximizing** the inner rate R_{in} as well as by **maximizing** the open EXIT tunnel area, since this allows the decoder to minimize the number of decoding iterations required, as explained further in the last paragraph of this section. The open EXIT-chart area is given by the square of the EXIT chart matching error function, which is expressed as:

$$J(\lambda_1, \cdots, \lambda_P) = \int_0^1 \mathbf{e}(\rho)^2 di, \tag{13}$$

where the error function is given by: $\mathbf{e}(\rho) =$

$$\underbrace{\begin{bmatrix} \Gamma_1(I_{A,1}), & \cdots & \Gamma_P(I_{A,1}) \\ \Gamma_1(I_{A,2}), & \cdots & \Gamma_P(I_{A,2}) \\ \vdots, & \ddots & \vdots \\ \Gamma_1(I_{A,l}), & \cdots & \Gamma_P(I_{A,l}) \end{bmatrix} \begin{bmatrix} \lambda_1 \\ \lambda_2 \\ \vdots \\ \lambda_P \end{bmatrix}}_{\Gamma_{in}} - \underbrace{\begin{bmatrix} \Gamma_{rsc}^{-1}(I_{A,1}) \\ \Gamma_{rsc}^{-1}(I_{A,2}) \\ \vdots \\ \Gamma_{rsc}^{-1}(I_{A,l}) \end{bmatrix}}_{\Gamma_{rsc}} \tag{14}$$

subject to the constraints imposed by Equation (11), where $I_{A,l}$ denotes the l-th *a-priori* information input of the PLDC components.

The gradient search method of maximizing $J(\lambda_1, \cdots, \lambda_P)$ of Equation (13) is similar to the algorithm proposed in [9]. More explicitly, the algorithm starts by setting the inner code rate R_{in} to the minimum value. If the set of weighting coefficients hosted by the vector $\boldsymbol{\lambda}$ is generated using the gradient search method of [9] for maximizing the area expression of Equation (13) and an open EXIT tunnel exists, R_{in} is increased by a small amount. The algorithm terminates at the highest possible R_{in} value, where an open convergence tunnel may no longer be found.

The reason that our proposed inner IR-PLDC scheme is seeking the solutions **maximizing** the area expression of $J(\lambda_1, \cdots, \lambda_P)$ is justified as follows. The benefit of employing irregular inner or outer codes for an iteratively-detected scheme is to maximize the achievable rate. When using IRCCs as an outer code, minimizing the EXIT tunnel area corresponds to maximizing the achievable rate, owing to the "area property" [13]. In other words, IRCCs aim for finding an outer EXIT curve that "matches" a given inner EXIT curve as close as possible by maximizing the area under the EXIT curve. By contrast, there is no one-to-one relationship between R_{in} of IR-PLDC and the area under the EXIT curves. Consequently, the IR-PLDC scheme offers multiple area values under its EXIT curves for any given rate R_{in}. Having a larger EXIT tunnel area potentially requires less iterations to achieve an infinitesimally low BER. Therefore, given an outer code, the design criterion for the inner IR-PLDC code is to **maximize the inner code rate R_{in} and simultaneously maximize the open EXIT tunnel area according to Equation (13)**.

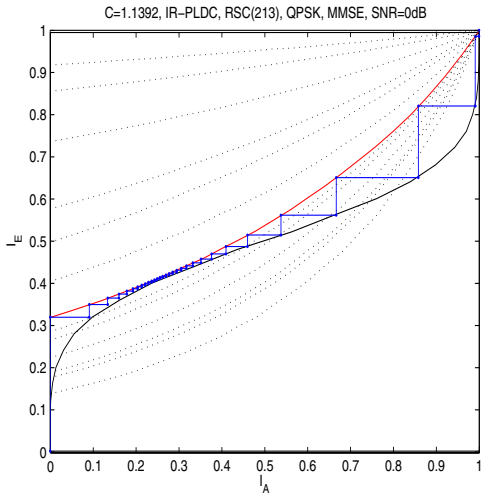

Figure 3. EXIT chart and the decoding trajectory of the RSC(213)-coded IR-PLDC scheme of Figure 1 recorded at $\rho = 0dB$ using QPSK modulation, when an MMSE detector was employed.

IV. SIMULATION RESULTS

In this section, we present the EXIT charts of the proposed RSC-coded IR-PLDC scheme designed for maximizing the throughput at a certain SNR value, as well as maintaining an infinitesimally low BER. Later, we will generalize the design process to a wide range of SNRs. Note that an interleaver length of 10^6 bits is employed for the first interleaver of Figure 1.

Figure 3 presents the EXIT chart and the corresponding decoding trajectory of our IR-PLDC scheme designed for operating at $\rho = 0dB$, when a half-rate RSC(213) code was employed as the outer code. The dotted lines represent the EXIT curves of the $P = 12$ component codes of Table I. Observe that the area under the component EXIT curve is increased when the rate is decreased, which corresponds to different component PLDCs having different maximum achievable rates. The shape of all the dotted curves is similar, since they are all combined with the IIR memory-1 precoders. The solid lines represents the EXIT curves of the outer RSC(213) code and of the IR-PLDC system having a weighting coefficient vector of:

$$\lambda = [0, 0, 0, 0, 0.82, 0.146, 0, 0, 0, 0.034, 0, 0].$$

The resultant total rate of the system is $C_{total} = R_{in} \cdot R_{out} \cdot (bits/sym) = 0.5 \cdot 1.1392 \cdot 2 = 1.1392$ (bits/sym/Hz). By simultaneously maximizing R_{in} and the EXIT tunnel area using Equation (13), the optimized EXIT curve of the IR-PLDC of Figure 3 exhibits a significant open tunnel area, where the decoding trajectory of Figure 3 shows that $k = 28$ outer iterations were required.

The corresponding BER of the IR-PLDC system designed for achieving an infinitesimally low BER at $\rho = 0dB$ in conjunction with the RSC(213) code using QPSK modulation is shown in Figure 4. There is a turbo cliff at $\rho = 0dB$, when $k = 28$ outer iterations were carried out between the RSC(215) code and IR-PLDC decoders. Given the number of outer iterations and the complexity of each PLDC component of Table I combined with the $RSC(213)$

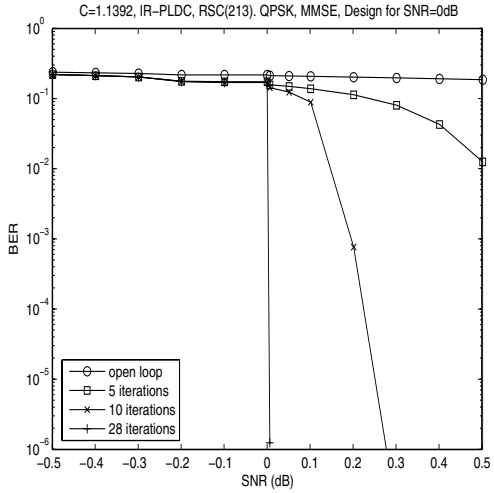

Figure 4. BER of the RSC(213)-coded IR-PLDC scheme of Figure 1 designed for achieving an infinitesimally low BER at $\rho = 0dB$ using QPSK modulation, when an MMSE detector was employed.

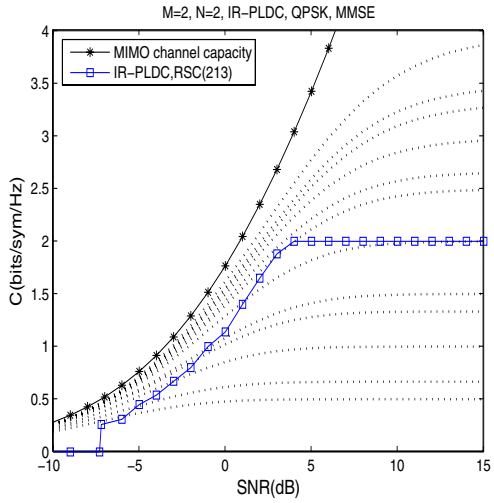

Figure 5. The maximum rates achieved by the IR-PLDC scheme of Figure 1 using an RSC(213) code, when QPSK modulation combined with an MMSE detector was employed.

code required a total of 217 ACS operations. The total decoding complexity per LLR value at $\rho = 0dB$ was evaluated by considering the number of iterations as well as each component's complexity, which is given by: $\varpi_{213}(0dB) = 28 \cdot (0.146 \cdot 8562 + 0.034 \cdot 18126 + 0.82 \cdot 12546 + 217) = 3.4639 \times 10^5$ (ACS).

Naturally, the same design process can be extended to other SNR values. Figure 5 plots the maximum rates achieved by the proposed IR-PLDC scheme of Figure 1, when the half-rate RSC(213) code was combined with QPSK modulation. Each point in Figure 5 was designed to achieve the maximum rate with the aid of the specific weighting coefficient vector $\boldsymbol{\lambda}$, which is not included here owing to the lack of space. The dotted lines in Figure 5 represent the DCMC capacity of the PLDC component codes of Table I plotted using Equation (9), which approach the MIMO channel's capacity, when we have larger Q values. The proposed RSC(213)-coded IR-PLDC scheme is capable of operating at a low BER for SNRs in excess of $\rho = -7$dB and operating as close as about 2.5dB to the MIMO channel's capacity, again maintaining an infinitesimally low BER. However, the achievable rate increase is limited to 2 (bits/sym/Hz) for SNRs in excess of $\rho = 4$dB, because the inner IR-PLDC scheme only supports a rate as high as $R_{in} = 2$, which was combined with a conventional half-rate RSC(213) code. Clearly, a further rate increase can be achieved, when higher-rate PLDC components are employed.

V. CONCLUSION

In this paper, we proposed a novel IR-PLDC scheme and demonstrated that it is capable of operating at about 2.5dB from the MIMO channel's capacity at a manageable complexity, when it was serially concatenated with a simple RSC(213) code. Furthermore, we have shown that the proposed irregular inner scheme becomes capable of reliably operating for SNRs in excess of -7dB, while maintaining an infinitesimally low BER. We also proposed a novel method of optimizing the component LDCs according to their DCMC capacity. The other coding blocks of Figure 1 and the choice of all the iterative decoding parameters were also optimized from a capacity maximization perspective with the aid of EXIT charts.

REFERENCES

[1] G. J. Foschini and M. J. Gans. On Limits of Wireless Communications in a Fading Environment when Using Multiple Antennas. *Wireless Personal Communications*, 6(3):311–335, 1998.

[2] I. E. Telatar. Capacity of multi-antenna Gaussian channels. *European Transactions on Telecommunications*, 10:585–595, 1999.

[3] L. Z. Zheng and D.N.C. Tse. Diversity and multiplexing: a fundamental tradeoff in multiple-antenna channels. *IEEE Transactions on Information Theory*, 49(5):1073–1096, 2003.

[4] B. Hassibi and B.M. Hochwald. High-rate codes that are linear in space and time. *IEEE Transactions on Information Theory*, 48(7):1804–1824, July 2002.

[5] R.W.Jr. Heath and A.J. Paulraj. Linear dispersion codes for MIMO systems based on frame theory. *Signal Processing, IEEE Transactions on [see also Acoustics, Speech, and Signal Processing, IEEE Transactions on]*, 50(10):2429–2441, October 2002.

[6] R. H. Gohary and T. N. Davidson. Design of linear dispersion codes: asymptotic guidelines and their implementation. *IEEE Transactions on Wireless Communications*, 4(6):2892–2906, November 2005.

[7] S. Benedetto, D. Divsalar, G. Montorsi, and F. Pollara. Serial concatenation of interleaved codes: performance analysis, design, and iterative decoding. *IEEE Transactions on Information Theory*, 44(3):909–926, 1998.

[8] O. Alamri, N. Wu, and L Hanzo. A differential turbo detection aided sphere packing modulated space-time coding scheme. *IEEE Vehicular Technology Conference*, 5:2474 – 2478, Spring 2006.

[9] M. Tüchler and J Hagenauer. Exit charts of irregular codes. *36th Conference on Information Sciences and Systems (CISS), (Princeton University)*, pages 20–22, 2002.

[10] M. Tüchler. Design of serially concatenated systems depending on the block length. *IEEE Transactions on Communications*, 52(2):209–218, February 2004.

[11] S. ten Brink, J. Speidel, and R. H. Yan. Iterative demapping and decoding for multilevel modulation. *IEEE Global Telecommunications Conference, GLOBECOM*, 1:579–584, November 1998.

[12] S. ten Brink. Designing iterative decoding schemes with the extrinsic information transfer chart. *AEÜ International Journal of Electronics and Communicatioons*, 54:389–398, 2000.

[13] A. Ashikhmin, G. Kramer, and S. ten Brink. Extrinsic information transfer functions: model and erasure channel properties. *IEEE Transactions on Information Theory*, 50(11):2657–2673, 2004.

[14] F. Brannstrom, L. K. Rasmussen, and A. J. Grant. Convergence analysis and optimal scheduling for multiple concatenated codes. *IEEE Transactions on Information Theory*, 51(9):3354–3364, September 2005.

[15] S. X. Ng and L. Hanzo. On the MIMO channel capacity of multi-dimensional signal sets. *IEEE Transactions on Vehicular Technology*, 55(2):528–536, March 2006.

[16] A. Ashikhmin, G. Kramer, and S. ten Brink. Code rate and the area under extrinsic information transfer curves. *IEEE International Symposium on Information Theory*, 1:115, 2002.